International Journal of Mineral Processing 157 (2016) 7–15

Contents lists available at ScienceDirect

International Journal of Mineral Processing

journal homepage: www.elsevier.com/locate/ijminpro

Synthesis of nanosized Cr_2O_3 from turkish chromite concentrates with sodium borohydride ($NaHB_4$) as reducing agent

Mehmet Hakan Morcali [a,*], Cagrı Eyuboglu [b], Serdar Aktas [b]

[a] Kahramanmaras Sutcu Imam University, Department of Environmental Engineering, 46100, Kahramanmaras, Turkey
[b] Marmara University, Engineering Faculty, Metallurgical & Materials Division, Goztepe Campus, Istanbul, Turkey

ARTICLE INFO

Article history:
Received 13 February 2015
Received in revised form 10 April 2016
Accepted 31 August 2016
Available online 1 September 2016

Keywords:
Chromium
Chromite Concentrate
Sodium Borohydride
Reduction

ABSTRACT

In this work, we investigated chromium extraction using a pyrometallurgical process and the subsequent production of nano-sized chromium oxide from Turkish chromite concentrate by assessing the effects of the base amount, fusion temperature, and fusion time on the chromium conversion. Nano-sized chromium oxide (Cr_2O_3) can be employed in many applications, such as catalysis, wear resistant materials, and advanced colorants, etc. To convert Cr(III) to Cr(VI) in the form of potassium chromate, potassium hydroxide (KOH) was employed under air flowing at a rate of 20.0 L/min. The kinetics of conversion from Cr(III) to Cr(VI) were also explored. Dissolution of the resulting potassium chromate in distilled water and pH neutralization afforded precipitation of aluminum hydroxide, which could be removed by filtration. The Cr(VI) in solution was subsequently converted to Cr(III) using sodium borohydride. The resulting chromium hydroxide was converted to nano-sized chromium oxide by heating at ambient pressure and temperatures between 1073 K and 1473 K. Heating to lower temperatures was found to be associated with a smaller particle size.

1. Introduction

Chromium is well-known for its significant corrosion resistance and is an important industrial metal used in various products and processes such as stainless steel production, textile dying, chemicals and pigments, and wood preservation. Chromium is also used in the tanning, electroplating, and refractory industries and for finishing metals, plastics, and leather. (Burch and Dolbear, 1918; Dennis and Such, 1993; Habashi, 1969; Kogel et al., 2006). Both its high resistance to corrosion and relatively high strength make chromium a valuable material for use in the mining industry (Gu and Wills, 1988). Producing chromium from chromite ore ($FeCr_2O_4$) is usually a multistep process involving one or more of the following unit operations: pyrometallurgical digestion, leaching with water, solution purification, filtration, crystallization (as sodium chromate or potassium chromate), and calcination (Burch and Dolbear, 1918; Gu and Wills, 1988; Papp, 2011). Recently, elimination of some of the latter intermediate steps has been investigated revealing that there is a potential to reduce energy consumption and decrease overall operating costs. However, no remarkable solution has been found to date (Aktas et al., 2015; Papp, 2011). Approximately 95% of the world's chromite ores are employed in the metallurgical industry as ferrochrome alloy (50–70% chromium in iron) (Kogel et al., 2006; Papp, 2011). Turkey has large amounts of chromite ore and is home to Eti Krom A.S., a leading local ferrochrome producer, and Kromsan, an esteemed worldwide leader in the chromium industry (Aktas et al., 2015). Recently, several studies have surfaced in the scientific literature on the dissolution of chromite ore using an oxidizing atmosphere. For instance, basic fusion reactions using sodium carbonate (Antony et al., 2001; Wang et al., 2007; Zhang et al., 2010b), calcium oxide (Sun et al., 2007, 2009), or sodium hydroxide (Aktas et al., 2015; Arslan and Orhan, 1997) have been described. Each method results in generally high efficiencies, though fusion with sodium carbonate and calcium oxide usually requires higher temperatures than necessary in hydroxide fusion. A disadvantage of calcium oxide fusion is the fact that the resulting $CaCrO_4$ product will dissociate into Ca(II) and highly toxic chromate ion in solution, thus further management is essential for recovery of chromium from these complex solutions (Sun et al., 2007, 2009; Zheng et al., 2006). In the present work, we present a method whereby chromite concentrate is converted to chromate via an oxidizing atmosphere in potassium hydroxide media, which requires a low fusion temperature and results in high yields of chromate.

There are documented methods of preparing Cr_2O_3 nanoparticles that include a precipitation, gelation process, microwave plasma, decomposition of chromium nitrate solution, and laser-induced deposition (Farzaneh, 2011; Kakaei-Lafdani and Aghaie-Khafri, 2012; Santulli et al., 2011; Wei et al., 2012), but due to the complex nature of these processes and the associated expensive equipment, these routes are also challenging to scale-up. Hydrometallurgical reduction of Cr(VI) in the presence of a base is a rapid and straightforward process that is as effective as alternatively using reducing agents such as ferrous sulfate, sulfur dioxide, or sodium bisulfate. This process readily affords

* Corresponding author.
E-mail address: hakanmorcali@gmail.com (M.H. Morcali).

http://dx.doi.org/10.1016/j.minpro.2016.08.018
0301-7516/

precipitation of chromium (III) as chromium hydroxide ($Cr(OH)_3$). When sulfur based reducing agents are employed, unwanted H_2S gas is produced, which has been observed by some researchers (Buerge and Hug, 1999; Hua and Deng, 2003). In this proposed process, this gas has not been evolved. On the other hand, sodium borohydride has not been reported in the scientific literature as a suitable base for this process, though it can easily reduce Cr(VI) to Cr(III) and also stimulate its precipitation as chromium hydroxide.

The primary purpose of this study was to investigate the effectiveness of a pyrometallurgical process for converting chromium from chromite concentrate, using potassium hydroxide (KOH) in the presence of air as an oxidizing agent. To evaluate the global activation energy for chromium reduction through a quantitative kinetic study of the reducing process in the presence of $NaHB_4$. Following isolation of potassium chromate from the above reaction and dissolution of the salt in water, the Cr(VI) was subsequently reduced to Cr(III) in the form of $Cr(OH)_3$ by addition of sodium borohydride. Subsequently, the $Cr(OH)_3$ was converted to nano-sized chromium oxide (Cr_2O_3) by heating at ambient pressure and various temperatures ranging from 1073 K to 1473 K. The products obtained were characterized using scanning electron microscopy (SEM).

2. Experimental methodology

Concentrated Turkish chromite was obtained from the Adıyaman Region in Turkey. The composition of the concentrate samples used are given in Table 1.

To determine the chemical composition, three samples of the chromite were analyzed for Cr, Mg, Fe, Al, and Si using redox-titration and an atomic absorption spectrometer (ContrAA 300; Analytik Jena AAS). The samples were prepared for analysis according to the following standard procedure: the concentrate was ground, sieved, and homogenized using a three-dimensional shaker.

The ore was decomposed by fusion with KOH + Air. After leaching in water and filtration step, the solution was acidified with nitric and sulfuric acids. After cooling, the chromate or Cr (VI) was reduced by the addition of a measured excess of a ferrous ammonium sulfate, and the excess was titrated with a permanganate solution. This redox-titration test method was intended to be used for compliance with compositional specifications for chromium oxide content in chromium-bearing ores (ASTM E342–11).

The X-ray powder diffraction technique using Cu-Kα radiation over an angle (2θ) range of 10 to 80° with the support of X'Pert High Score plus software was used for characterization of phases present in the chromite ore. The peaks were compared with the software database and these corresponded to the references therein (ICDD reference: 01–079-5893). The mineralogical analysis of the chromite concentrate is shown on Fig. 1. It can be seen that the mineral is a complex solid solution of the pure spinel end members ($(Fe_{0.429}Mg_{0.616})(Cr_{0.475}Al_{0.495})_2O_4$) (Sun et al., 2007, 2009; Zhang et al., 2010a, 2010b).

Fig. 2 illustrates the process used to produce nano-sized chromium oxide.

The effects of reaction time, temperature, and amount of potassium hydroxide were evaluated during the oxidation of the Cr(III) from chromite to Cr(VI). Air, at a rate of 20.0 L/min, was blown through a copper pipe to an iron crucible where the chromite concentrate was placed.

Table 1
Composition of chromite concentrate used in the study.

Compounds	Mass, %
Cr_2O_3	48.88
MgO	15.56
FeO	17.6
Al_2O_3	15.28
SiO_2	2.63
Cr_2O_3/ FeO	2.77
Others	0.05

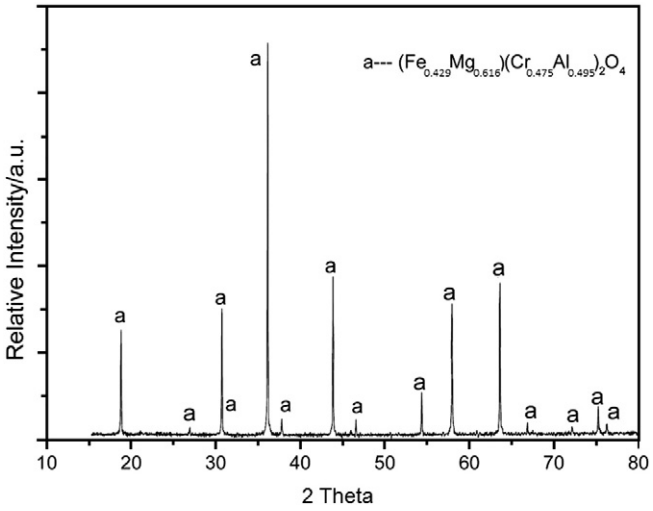

Fig. 1. The X-ray powder diffraction pattern of the chromite concentrate used in the study compare well with the ICDD reference: 01–079-5893.

The chromite concentrate (−75 + 45 μm) and variable amounts of potassium hydroxide (KOH) were fused for 15 to 120 min in the temperature range between 773 K and 973 K. To investigate the conversion behavior of chromium from the concentrate, a kinetic study was also undertaken at the same temperatures.

Conversion was calculated based on the amount of Cr(VI) formed via oxidation of the Cr(III) from the chromite concentrate:

$$\text{Conversion } (\%) = [M_{Cr6+}\ (g)/(W\ (g) \times 0.3345)] \times 100, \quad (1)$$

Where, M_{Cr6+} is the quantity of hexavalent chromium dissolved in the solution in grams, W is the sample weight in grams, and 0.3345 is the measured fraction of chromium content in the ground chromite concentrate.

After heating the chromite and KOH mixture under a flow of ambient air, the resulting solid cake was dissolved in distilled water to remove insoluble Fe(III) oxide (Fe_2O_3), and magnesium oxide (MgO). A series of trials added to the resulting basic solution to adjust the pH to 7, which facilitated the precipitation and removal of aluminum hydroxide ($Al(OH)_3$) to obtain a pure potassium chromate solution. Addition of sodium borohydride ($NaBH_4$) to this pure solution resulted in nano-sized chromium hydroxide ($Cr(OH)_3$). The advantage of using $NaBH_4$ is that this reagent effects both the reduction of Cr(VI) to Cr(III) and the formation of $Cr(OH)_3$. A series of trials was also performed to determine the optimum pH for precipitating $Cr(OH)_3$. The conversion to $Cr(OH)_3$ has been calculated using Eq. (2), based on the non-precipitated chromium present in the solution as detected using an atomic absorption spectrometer (ContrAA 300; Analytik Jena AAS) with standard protocol.

$$Cr(OH)_3\ (\%) = [(C_T - C_M)/C_T] \times 100 \quad (2)$$

Where C_T represents the initial concentration of the solution and C_M is final concentration of the solution.

During calcination of $Cr(OH)_3$ to Cr_2O_3, the temperature was varied over the range of 1073 K to 1473 K to determine the effect of temperature on particle size, which was measured using SEM. All chemicals used in this study were of analytical grade (Merck, Germany).

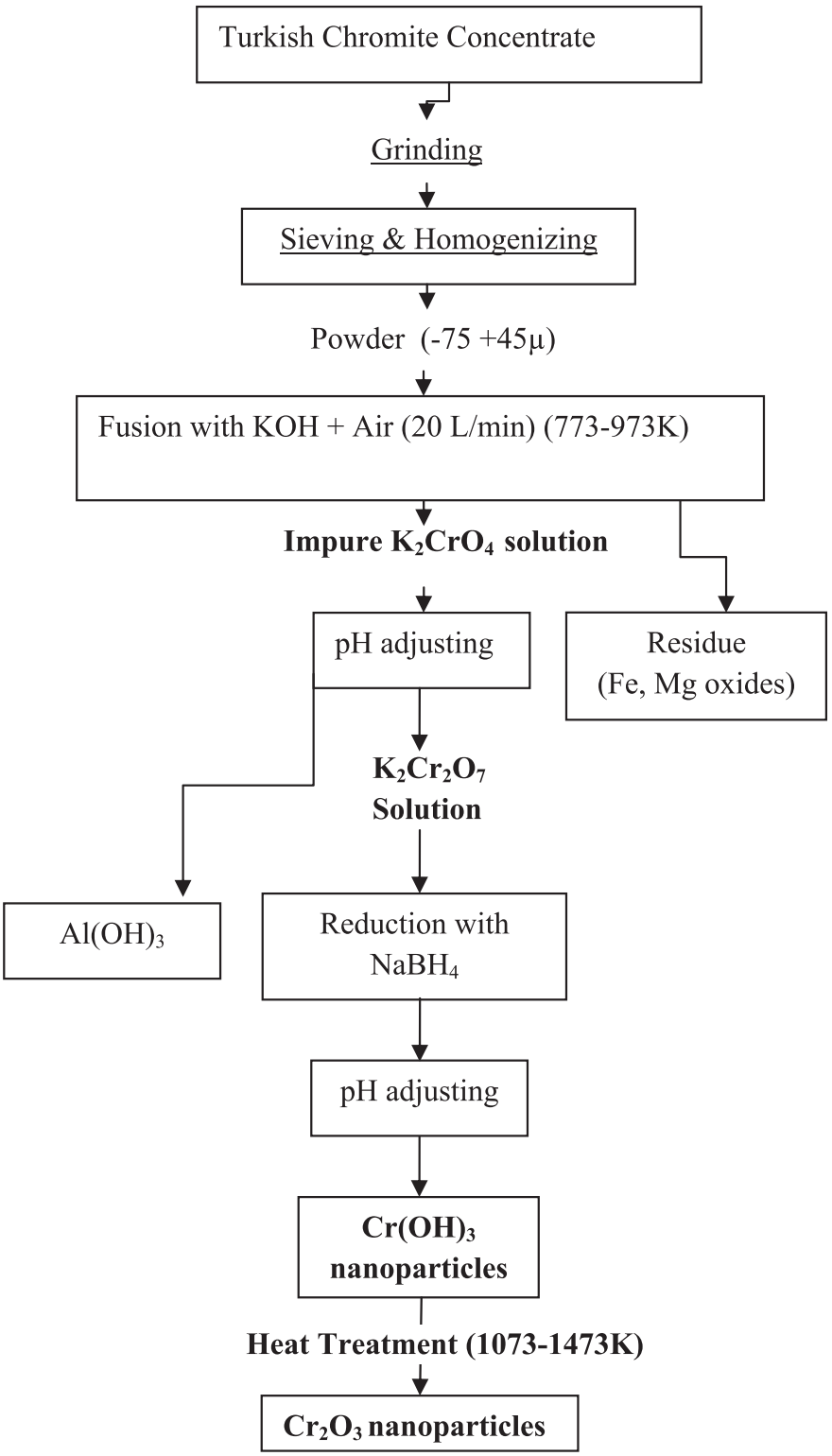

Fig. 2. Flow sheet for the process applied in the study.

3. Results and Discussion

The process of fusing the chromite with potassium hydroxide + air was successfully used to convert almost all the chromium from the chromite concentrate into a water-leachable Cr(VI) salt, potassium chromate. Other side products formed during chromium oxidation, such as $Al(OH)_3$, were removed by neutralizing the pH using sulfuric acid. The Cr(VI) solution was subsequently converted to Cr(III) in the form of chromium hydroxide upon the addition of sodium borohydride. Finally, heating of the obtained $Cr(OH)_3$ at various temperatures afforded its conversion to nano-sized chromium oxide.

3.1. Effect of the amount of KOH on chromium extraction

The chromite concentrate was fused with KOH above 773 K under a flow of ambient air in order to oxidize Cr(III) to Cr(VI). In all trials, air

flow was maintained at 20.0 L/min while the quantity of potassium hydroxide was varied (Aktas et al., 2015; Antony et al., 2001; Chen et al., 2013; Sun et al., 2009).

During fusion, the following reactions took place:

$$2FeCr_2O_4 + 8KOH + 7/2O_2 \rightarrow Fe_2O_3 + 4K_2CrO_4 + 4H_2O \quad (3)$$

$$MgCr_2O_4 + 4KOH + 3/2O_2 \rightarrow MgO + 2K_2CrO_4 + 2H_2O \quad (4)$$

$$2FeAl_2O_4 + 4KOH + 1/2O_2 \rightarrow Fe_2O_3 + 4KAlO_2 + 2H_2O \quad (5)$$

Fig. 3 is a plot of conversion versus the quantity of KOH used. As can be seen from this figure, the conversion increased with increasing amounts of potassium hydroxide until a threshold value of about 0.8 g, above which the chromium conversion did not increase. Previous studies on the oxidation of Cr(III) to Cr(VI) using similar routes have found that temperature plays a more important role than the amount of KOH, for instance a temperature of 873 K was found to be insufficient for complete extraction of chromium (Aktas et al., 2015; Chen et al., 2013; Sun et al., 2009). In order to further examine the role of temperature on the conversion efficiency, we carried out fusion reactions while varying the temperature between 773 K and 973 K.

3.2. Effect of fusion temperature on chromium extraction

In this series of experiments, the effects of fusion time and temperature on conversion were investigated. As shown on Fig. 4, temperature plays a major role in disruption of the spinel lattice and the subsequent conversion process (Xu et al., 2006; Yarkadaş and Yildiz, 2009). This effect is also more pronounced at higher KOH quantities. When 3 g KOH was employed, the chromium conversion was 57% and 83% at 773 K and 973 K, respectively. It should be noted that an increase of temperature from 773 K to 973 K, led to a further increase in recovery by approximately 46%, which suggests that temperature plays a significant role in chromium extraction from this concentrate and is a trend that agrees with previous reports in the literature (Arslan and Orhan, 1997; Sun et al., 2007; Xu et al., 2005; Zhang et al., 2010b; Zheng et al., 2006). Notably, an increase in temperature from 923 K to 973 K results in a negligible difference in chromium conversion. It is also evident from the data on Fig. 4 that it is possible to extract chromium at levels as high as 91% when the reaction is carried out at 923 K for 1 h using a 5:1 (*w*/w) KOH:chromite ratio. The optimal conversion with this particular ratio of reagents results from the fact that the conversion reaction is diffusion controlled, as evidenced by a detailed study of the reaction kinetics (vide infra). Sufficient potassium hydroxide and reaction time were

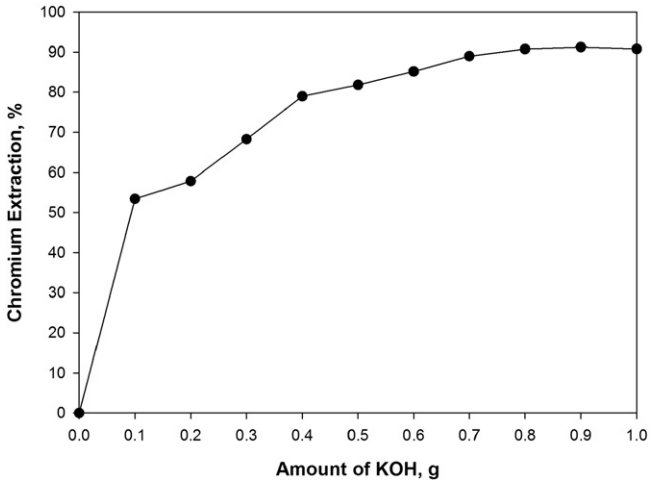

Fig. 3. Change in extraction (%) of Cr with regard to the KOH amount (1 g conc., 873 K, 60 min).

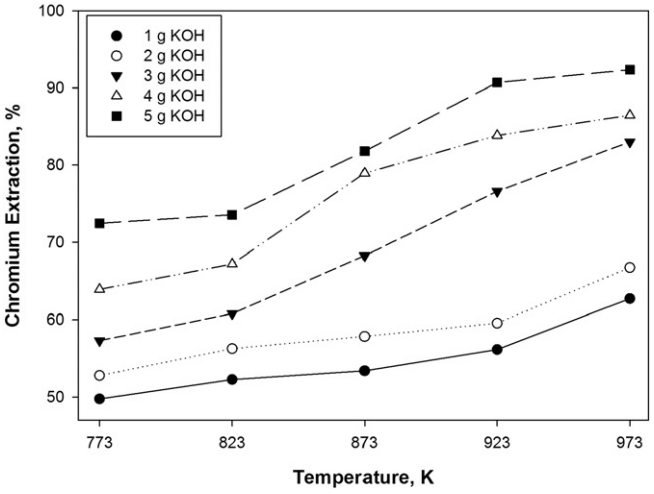

Fig. 4. Effect of temperature on the conversion of chromium (60 min, 1 g conc.).

therefore necessary to promote the observed improvement in the conversion.

3.3. Effect of fusion time on chromium extraction

We also examined the effect of reaction time on the conversion of Cr(III) to Cr(VI) when 2 g KOH was used with (2:1 (w/w) KOH:chromite ratio) 1 g of chromite at a fusion temperature of 923 K. As shown on Fig. 5, longer fusion times are important to promote chromium conversion. For instance, 49% of the chromium was converted after 15 min of fusion at 923 K. When fusion time was extended to 1 h, however, the conversion rose to 88%. Thus, both elevated temperatures and increased fusion times contribute to an overall enhancement in chromium conversion (Aktas et al., 2015). It is worth noting that conversion leveled off after 90 min of fusion, suggesting that there is no need for extended period of fusion time.

3.4. Kinetics of extraction of chromium from chromite concentrate

A kinetic model can be determined by extracting the reaction order from experimental data using either a differential rate law or an integrated rate law. We studied the chromium conversion to identify the underlying kinetics from a body of possible conversion mechanisms, such as one-, two-, or three-dimensional diffusion and even a simple first order mechanism. The reaction models and the corresponding

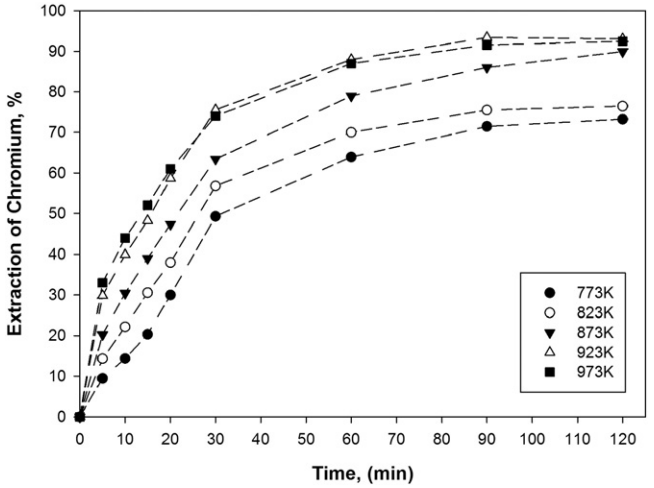

Fig. 5. Effect of time on the conversion of chromium (2 g of KOH, 1 g conc.).

Table 2
Conversion percentages of Cr (VI) depending on pH level of the solution.

pH	Cr (IV) (mg)	$NaBH_4$ (mg)	Cr (VI)* (mg)	Cr (III)* (mg)	Conversion, %
6.03	26.77	20	16.71	10.06	37.59
7	26.77	20	14.34	12.43	46.42
8.15	26.77	20	15.21	11.56	50.08
8.9	26.77	20	10.42	16.35	61.07
9.88	26.77	20	9.82	16.95	63.31
11.01	26.77	20	8.32	18.45	68.93
12.03	26.77	20	4.18	22.59	84.37

* after employed with $NaBH_4$.

kinetic equations that were applied are given in Table 3. In each kinetic experiment, several mathematical models were applied for temperatures ranging from 773 K to 923 K and the corresponding model curves were compared with the experimental kinetic data (these model curves are not shown). The R^2 values of the kinetic models shown that the diffusion of reactants in the layer best fitted kinetic model in our results (Table 2).

$$t = 1 + 2\,(1-X) - 3\,(1-X)^{2/3} \tag{6}$$

To determine the rate constant (k) of chromium conversion between 773 K and 923 K, $1 + 2\,(1-X) - 3\,(1-X)^{2/3}$ was plotted versus time as shown on Fig. 6. Here X denotes the fraction of chromium conversion (Chen et al., 2013; Zhang et al., 2010b). The activation energy, E_a, was then calculated using the Arrhenius equation:

$$k = Ae^{-Ea/RT} \text{ or } \ln k = \ln A - E_a/RT \tag{7}$$

where, k is the rate constant of the extraction process, R is the ideal gas constant, and T is the temperature in Kelvin.

The Arrhenius plot of ln k versus $1000/T$ is given on Fig. 7. From the slope of the best linear fit to the data the activation energy for the chromium extraction was determined to be 73.78 ± 3.54 kJ/mol, The result revealed that the chromium extraction is controlled by mass diffusion in the product layer which is consistent with other reports in the literature (Chen et al., 2013; Zhang et al., 2010b).

3.5. Nano-sized chromium oxide production using sodium borohydride

After the Cr(VI) was extracted into solution as potassium chromate, the pH was adjusted to 7 to promote precipitation of $Al(OH)_3$. Subsequently, a diluted $NaBH_4$ solution was added to the resulting pure K_2CrO_4 solution to ensure that all Cr(VI) was converted to Cr(III)

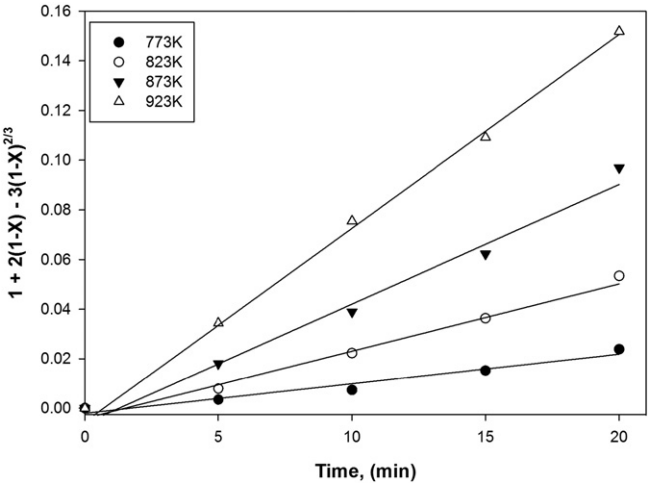

Fig. 6. Plot of $1 + 2(1\text{-}X)\text{-}3(1\text{-}X)^{2/3}$ with respect to time.

(Alidokht et al., 2011; Patnaik, 2004) according to the following balanced chemical equation:

$$K_2CrO_4 + NaBH_4 + 5H_2O \rightarrow Cr(OH)_3 + NaOH + 2KOH + H_3BO_3 + 5/2H_2 \tag{8}$$

As shown on Fig. 8, sodium borohydride is more effective as a reducing agent at elevated pH levels. For example, at a pH of 6.03 the conversion was below 40% while increasing the pH to 12.03 almost double the amount of Cr(III) generated during reduction. It should also be noted that for this conversion, a substoichiometric amount of sodium borohydride (20 mg) was employed to demonstrate this effect. An advantage of using sodium borohydride for this reaction is that both the Cr(VI) reduction and precipitation of $Cr(OH)_3$ take place in one experimental step. This facile route is in contrast to most industrial applications wherein Cr(VI) is converted to Cr(III) in acidic media and then chromium hydroxide is subsequently precipitated by addition of a base to the acidic solution. By using sodium borohydride, the need to add a basic reagent for hydroxide formation is eliminated. It should be noted that if the conversion is carried out in basic media (e.g. a solution of sodium hydroxide), then even less sodium borohydride is needed. Table 2 shows the conversion of Cr(VI) at various pH values.

We also investigated the effect of pH on the extent of $Cr(OH)_3$ precipitation. For this experiment sodium hydroxide was added to a solution of chromium sulfate ($Cr_2(SO_4)_3$) with an initial pH of 3, and the pH was recorded along with the fraction of solid $Cr(OH)_3$ formed at various intervals. Fig. 9 displays the fraction of chromium hydroxide precipitated versus the corresponding pH. For low pH values the fraction of isolated $Cr(OH)_3$ was correspondingly low, while at higher pH values

Table 3
The studied kinetic equations.

Reaction model	Kinetic equations	R^2 Values at different temperature (K)			
		773	823	873	923
Diffusion of reactants in the layer	$1 + 2(1\text{-}X)\text{-}3(1\text{-}X)^{2/3} = kt$	0.995	0.991	0.992	0.994
Shrinking core	$1\text{-}(1\text{-}X)^{1/3} = kt$	0.860	0.843	0.835	0.826
One-dimensional diffusion	$\times^2 = kt$	0.775	0.792	0.783	0.791
Two-dimensional diffusion	$(1\text{-}X)\ln(1\text{-}X) + X = kt$	0.860	0.854	0.872	0.864
Ginstling–Brounshtein equation, three-dimensional diffusion	$1\text{-}(2/3)X\text{-}(1\text{-}X)^{2/3} = kt$	0.850	0.861	0.849	0.826
Jander equation, three-dimensional diffusion	$[1\text{-}(1\text{-}X)^{1/3}]^2 = kt$	0.769	0.725	0.751	0.746
First-order kinetics	$-\ln(1\text{-}X) = kt$	0.821	0.804	0.831	0.815
Two-dimensional phase boundary reaction	$1\text{-}(1\text{-}X)^{1/2} = kt$	0.843	0.869	0.824	0.796
Three-dimensional phase boundary reaction	$1\text{-}(1\text{-}X)^{1/3} = kt$	0.824	0.769	0.758	0.771
Random nucleation: Avrami equation	$[-\ln(1\text{-}X)]^{1/2} = kt$	0.724	0.678	0.694	0.713
Random nucleation: Erofeev equation	$[-\ln(1\text{-}X)]^{1/3} = kt$	0.788	0.812	0.759	0.789

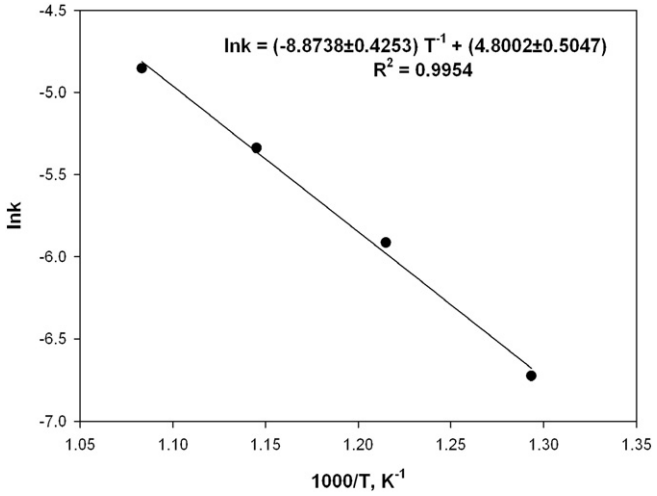

Fig. 7. Arrhenius plot of ln k vs. 1000/T.

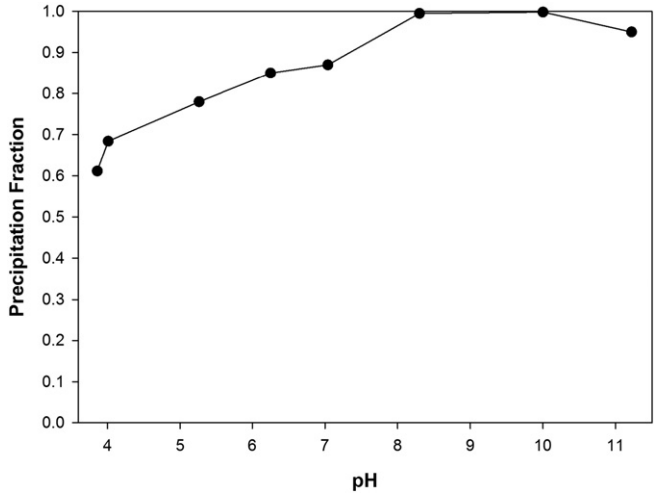

Fig. 9. Precipitation fraction of chromium hydroxide via sodium hydroxide as a function of the solution pH containing 1000 ppm $Cr_2(SO_4)_3$.

it was possible to isolate more $Cr(OH)_3$ precipitate. A maximum amount of precipitate was obtained between pH values of 8.2 and 10 (see Fig. 9). $Cr(OH)_3$ has an amphoteric character, dissolving in acidic solutions to form $[Cr(H_2O)_6]^{3+}$ and in basic solutions to form $[Cr(OH)_6]^{3-}$ (Ebbing and Gammon, 2010). This increase in precipitation with increasing pH can be rationalized by considering that as excess OH^- begins to accumulate in solution it will promote the formation of $Cr(OH)_3$ thermodynamically and kinetically.

Interestingly, it was observed that nano-sized particles of $Cr(OH)_3$ were preferentially precipitated because the Cr(III) ions began to precipitate under only slightly basic pH. This is in contrast to Cr(VI), which is stable in solution and does not precipitate over the entire range of investigated pH values (Fig. 9).

3.6. Characterization of the obtained $Cr(OH)_3$ and Cr_2O_3 powders

The morphology of the precipitated chromium hydroxide was also studied using SEM. The corresponding images are shown on Fig. 10 and illustrate the nano-sized $Cr(OH)_3$ particles that were obtained with a particle size ranging in the range between 30 nm to 80 nm.

After precipitation of $Cr(OH)_3$, calcination was carried out to produce Cr_2O_3 containing powder. Potentiometric titration was then used to determine the purity of the Cr_2O_3 powder obtained. The sample

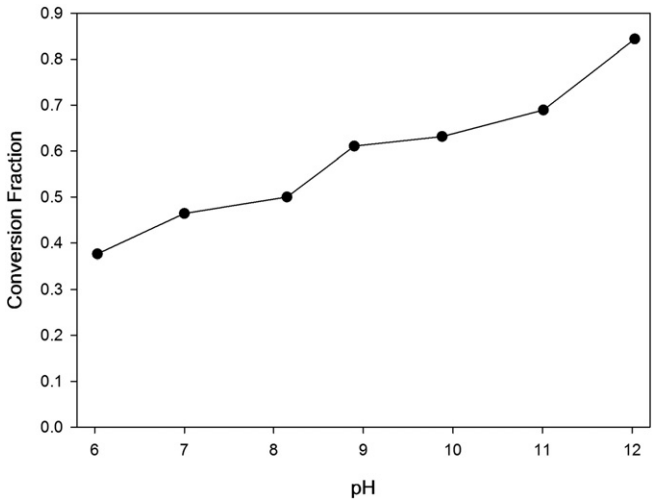

Fig. 8. Conversion fraction of chromium (VI) to (III) via sodium borohydride.

was found to contain 99.85% chromium oxide and the full chemical analysis is given in Table 4.

SEM images were also obtained for the chromium oxides nanoparticles obtained under varying calcination temperatures, and these are shown on Fig. 11. For comparison, Fig. 10a-b show the images of the precipitated chromium hydroxide precursor particles and Fig. 11a-e, respectively, show the associated Cr_2O_3 nanoparticles formed upon heating. As seen in particular on Fig. 10a and b, the $Cr(OH)_3$ particles exhibited a somewhat irregular shape with a wide size distribution ranging from 30 nm to 80 nm. Following calcination at 1073 and 1173 K, however, the precursor decomposed to loosely agglomerated Cr_2O_3 nanoparticles in an approximately round shape, as seen on Fig. 11a and b. A higher calcination temperature of 1373 and 1473 K weakened this agglomeration of nanoparticles, however, as seen in the comparison of Fig. 11d and e. This increase in particle agglomeration with higher calcination temperatures is consistent with other reports in the literature (Farzaneh, 2011; Kakaei-Lafdani and Aghaie-Khafri, 2012; Santulli et al., 2011; Wei et al., 2012). When weighing the costs associated with enhanced heat treatments, it is clear there is no need to use higher temperatures as reported previously because efficient thermal decomposition takes place at around 1073 K (Aktas et al., 2015; Santulli et al., 2011; Wei et al., 2012). This tendency has also been confirmed previously using Thermal Gravimetric Analysis (Aktas et al., 2015). On Table 5 particle size ranges for precipitates calcinated between 1073 K and 1473 K are presented and from this data it can be seen that particle size increases with increasing temperature. The particle sizes between 300 nm and 600 nm were achieved for calcination carried out at 1473 K.

4. Conclusions

In this study, a chemical processing scheme for producing nano-sized chromium oxide from Turkish chromite concentrate has been proposed, with the aim of identifying optimum dissolution, redox conversion, and calcination parameters. It was found that it is possible to extract Cr(III) from chromite concentrate at conversion levels exceeding 90% when the extraction is carried out by heating a 5:1 (*w*/w) mixture of KOH:chromite at 923 K for 1 h under a 20.0 L/min flow of air. It is worthwhile to mention that chromium extraction could be further enhanced through use of pure O_2 instead of air flow, thereby contributing for the oxidation potential of the atmosphere in contact with the sample. Kinetic modeling revealed that, under the imposed experimental conditions, the conversion of chromite to chromate is controlled by mass diffusion in the product layer with an activation energy of 73.78 ± 3.54 kJ/mol. The dissolved aluminum in the as-isolated

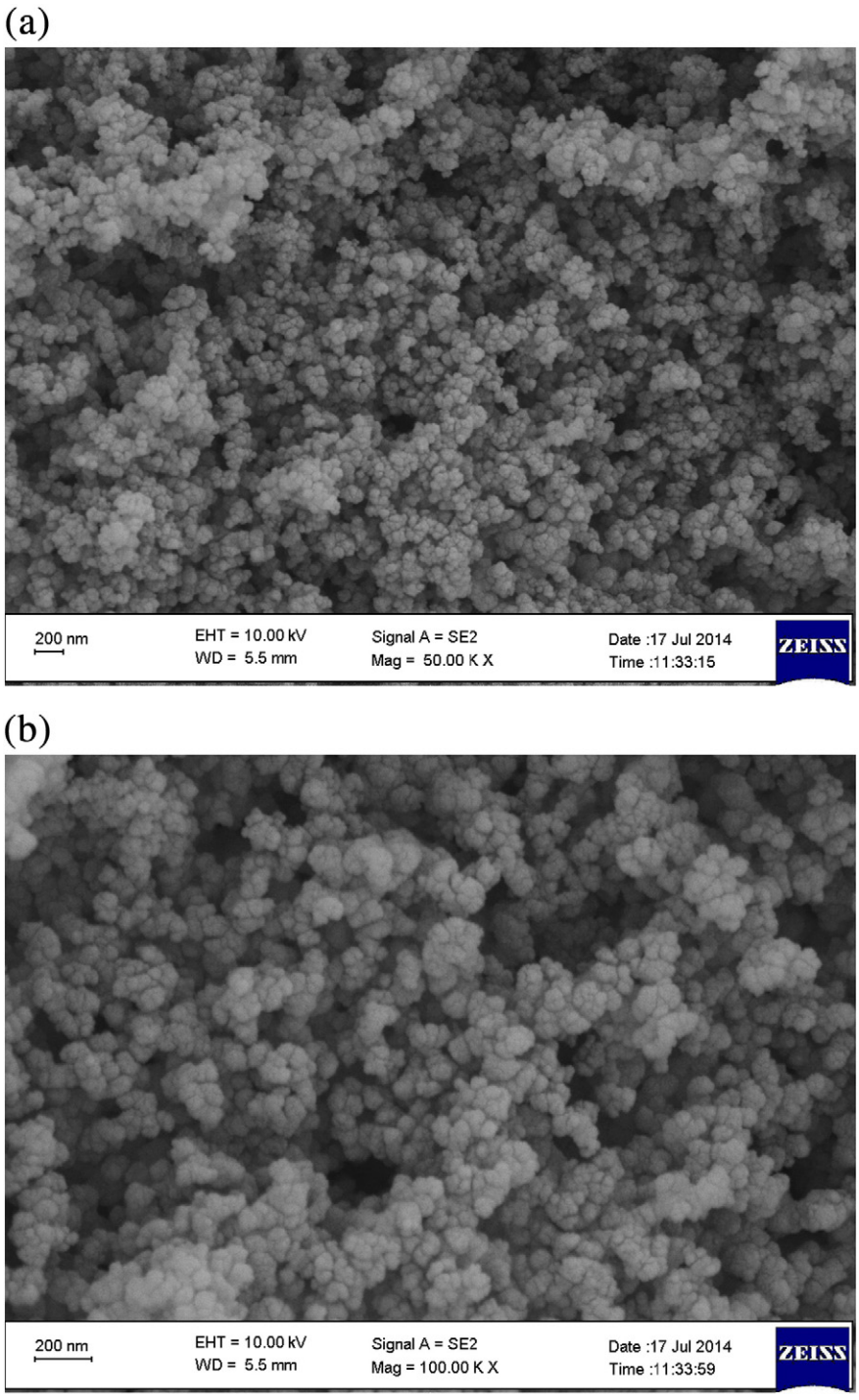

Fig. 10. SEM images of Chromium hydroxide with sodium borohydride (a) 50,000 X and (b) 100,000 X.

Table 4
Chemical analysis of obtained chromium oxide.

Compounds	Mass, %
Cr_2O_3	99.85
MgO	N/A*
Fe_2O_3	N/A*
Al_2O_3	0.04
SiO_2	0.02
Na_2O	0.09

* Not Available.

potassium chromate solution could be selectively precipitated as $Al(OH)_3$ by addition of H_2SO_4 at room temperature to bring the solution to a pH of 7. The Cr(VI) remaining in the resulting solution was subsequently converted to Cr(III) and then precipitated as chromium hydroxide in one experimental step through the addition of sodium borohydride. Finally, heating of the as-isolated chromium hydroxide to temperatures between 1073 K and 1473 K resulted in the formation of nanoparticles of Cr_2O_3, with lower temperatures promoting the formation of smaller particle sizes. The resulting Cr_2O_3 nanoparticles can be used in many products such as catalysts, wear resistant materials, and advanced colorants.

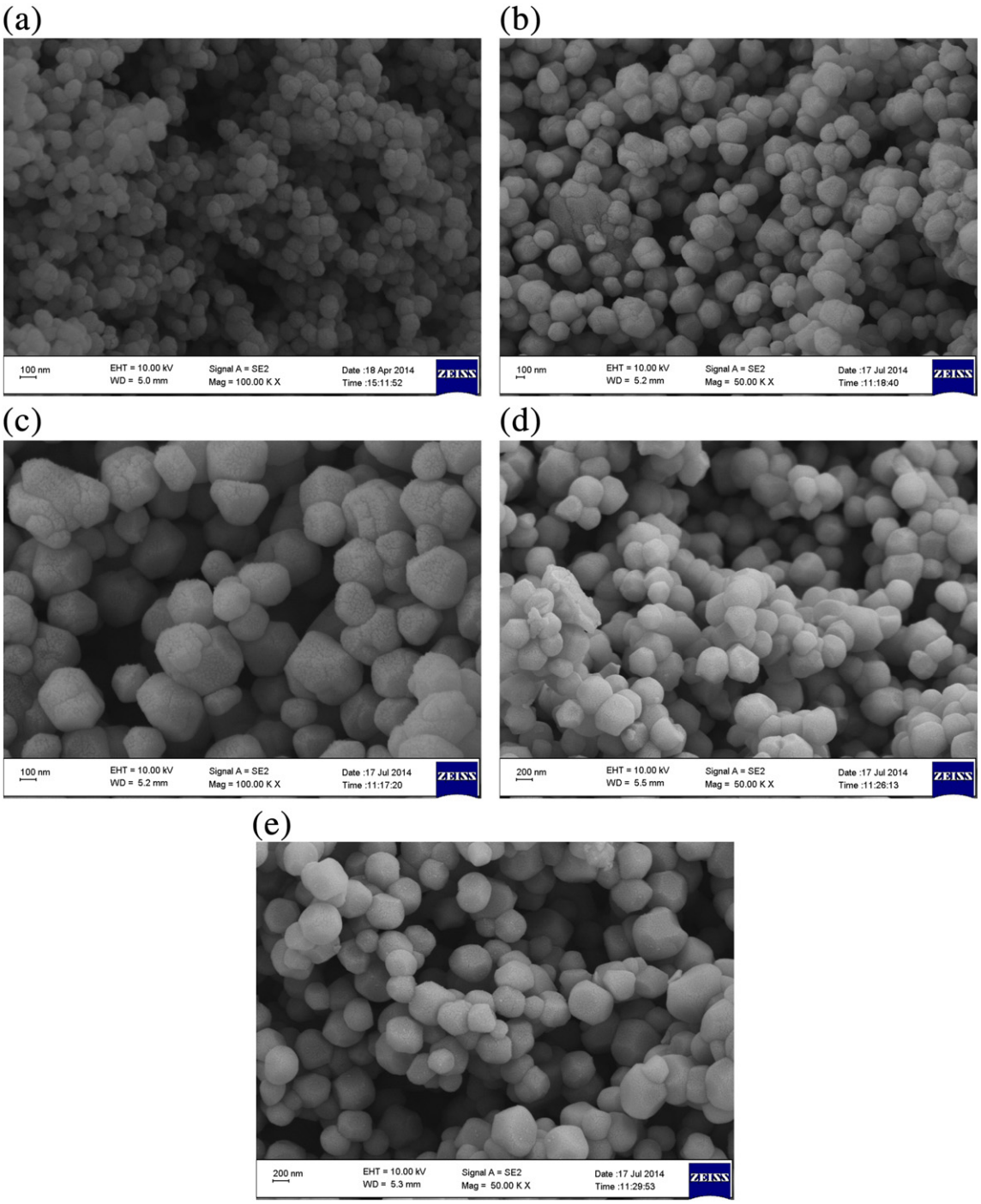

Fig. 11. SEM images of Chromium oxide after heat treatment at (a) 1073 K (b) 1173 K (c) 1273 K (d) 1373 K and (e) 1473 K.

Acknowledgements

The authors wish to thank Marmara Bapko for financial support under project FEN-E-150513-0121. Special thanks are due to Kromsan for providing valuable information regarding the process that is being applied.

Table 5
Particle size ranges at various temperatures.

Temperature (°K)	Particle size (nm)
1073	70–120
1173	171–265
1273	223–413
1373	294–447
1473	300–611

Appendix A. Supplementary data

Supplementary data to this article can be found online at http://dx.doi.org/10.1016/j.minpro.2016.08.018.

References

Aktas, S., Eyuboglu, C., Morcali, M., Özbey, S., Sucuoglu, Y., 2015. Production of Chromium Oxide from Turkish Chromite Concentrate Using Ethanol. High Temp. Mater. Processes 34, 237–244.

Alidokht, L., Khataee, A.R., Reyhanitabar, A., Oustan, S., 2011. Reductive removal of Cr(VI) by starch-stabilized Fe0 nanoparticles in aqueous solution. Desalination 270, 105–110.
Antony, M., Tathavadkar, V., Calvert, C., Jha, A., 2001. The soda-ash roasting of chromite ore processing residue for the reclamation of chromium. Metall. Mater. Trans. B Process Metall. Mater. Process. Sci. 32, 987–995.
Arslan, C., Orhan, G., 1997. Investigation of chrome (VI) oxide production from chromite concentrate by alkali fusion. Int. J. Miner. Process. 50, 87–96.
Buerge, I.J., Hug, S.J., 1999. Influence of mineral surfaces on chromium (VI) reduction by iron (II). Environ. Sci. Technol. 33, 4285–4291.
Burch, A., Dolbear, S.H., 1918. Chromite. Mining and Scientific Press.
Chen, G., Wang, J., Wang, X., Zheng, S.L., Du, H., Zhang, Y., 2013. An investigation on the kinetics of chromium dissolution from Philippine chromite ore at high oxygen pressure in KOH sub-molten salt solution. Hydrometallurgy 139, 46–53.
Dennis, J.K., Such, T.E., 1993. Nickel and chromium plating. Woodhead Publishing.
Ebbing, D., Gammon, S., 2010. General Chemistry. Enhanced edition. Cengage Learning 0-53849752-1.
Farzaneh, F., 2011. Synthesis and Characterization of Cr2O3 Nanoparticles with Triethanolamine in Water under Microwave Irradiation. J. Sci. Islam. Repub. Iran 22, 329–333.
Gu, F., Wills, B.A., 1988. Chromite- mineralogy and processing. Miner. Eng. 1, 235–240.
Habashi, F., 1969. Principles of extractive metallurgy. CRC Press.
Hua, B., Deng, B., 2003. Influences of water vapor on Cr (VI) reduction by gaseous hydrogen sulfide. Environ. Sci. Technol. 37, 4771–4777.
Kakaei-Lafdani, M.H., Aghaie-Khafri, M., 2012. Synthesis of high specific surface area Cr2O3 nanopowder. Micro Nano Lett. 7, 1072–1075.
Kogel, J.E., Trivedi, N.C., Barker, J.M., 2006. Industrial Minerals and Rocks: Commodities, Markets, and Users. SME.
Papp, J.F., 2011. Chromium. In Mineral commodity summaries. 2011 Minerals Yearbook. U.S. Geological Survey.
Patnaik, P., 2004. Dean's analytical chemistry handbook. McGraw-Hill New York.
Santulli, A.C., Feygenson, M., Camino, F.E., Aronson, M.C., Wong, S.S., 2011. Synthesis and Characterization of One-Dimensional Cr2O3 Nanostructures. Chem. Mater. 23, 1000–1008.
Sun, Z., Zheng, S.-l., Xu, H.-b., Zhang, Y., 2007. Oxidation decomposition of chromite ore in molten potassium hydroxide. Int. J. Miner. Process. 83, 60–67.
Sun, Z., Zhang, Y., Zheng, S.L., Zhang, Y., 2009. A new method of potassium chromate production from chromite and KOH-KNO3-H2O binary submolten salt system. AICHE J. 55, 2646–2656.
Wang, T., He, M., Pan, Q., 2007. A new method for the treatment of chromite ore processing residues. J. Hazard. Mater. 149, 440–444.
Wei, G.Y., Qu, J.K., Zheng, Y.D., Qi, T., Guo, Q., 2012. Preparation of Cr2O3 precursors by hydrothermal reduction in the abundant Na2CO3 and Na2CrO4 solution. Int. J. Miner. Metall. Mater. 19, 978–985.
Xu, H.B., Zheng, S.L., Zhang, Y., Li, Z.H., Wang, Z.K., 2005. Oxidative leaching of a Vietnamese chromite ore in highly concentrated potassium hydroxide aqueous solution at 300 °C and atmospheric pressure. Miner. Eng. 18, 527–535.
Xu, H.-B., Zhang, Y., Li, Z.-H., Zheng, S.-L., Wang, Z.-K., Qi, T., Li, H.-Q., 2006. Development of a new cleaner production process for producing chromic oxide from chromite ore. J. Clean. Prod. 14, 211–219.
Yarkadaş, G., Yildiz, K., 2009. Effects of mechanical activation on the soda roasting of chromite. Can. Metall. Q. 48, 69–72.
Zhang, Y., Zheng, S.-L., Du, H., Xu, H.-B., Zhang, Y., 2010a. Effect of mechanical activation on alkali leaching of chromite ore. Trans. Nonferrous Metal. Soc. 20, 888–891.
Zhang, Y., Zheng, S.-l., Xu, H.-b., Du, H., Zhang, Y., 2010b. Decomposition of chromite ore by oxygen in molten NaOH–NaNO3. Int. J. Miner. Process. 95, 10–17.
Zheng, S., Zhang, Y., Li, Z., Qi, T., Li, H., Xu, H., 2006. Green metallurgical processing of chromite. Hydrometallurgy 82, 157–163.